Monte Carlo simulation of a planar lattice model with P_4 interactions

Abhijit Pal and Soumen Kumar Roy
Department of Physics, Jadavpur University, Calcutta 700 032, India
(Received 17 May 2002; revised manuscript received 14 November 2002; published 28 January 2003)

Monte Carlo study of a two-dimensional lattice with three-dimensional spins ($d=2,n=3$) interacting with nearest neighbors via a $-P_4(\cos\theta)$ potential, where P_4 is the fourth Legendre polynomial and θ is the angle between two spins, has been reported for lattice sizes ranging from 10×10 to 160×160. A cluster algorithm for spin updating with a histogram reweighting technique has been used and finite size scaling has been performed. The model exhibits a strong first order phase transition at a dimensionless temperature 0.376 ± 0.015. The phase transition appears to be driven by condensation of topological defects and the defect density D increases sharply at the transition temperature. The temperature derivative dD/dT^* is found to obey a linear scaling relation with the lattice size L. The behavior of the model seems to be remarkably different from the two-dimensional P_2 model, that has been investigated by other authors, although both models possess the same symmetry and topological defects play an important role in the phase transition.

DOI: 10.1103/PhysRevE.67.011705 PACS number(s): 61.30.Gd

I. INTRODUCTION

The n-vector $O(n)$ models in two dimension are defined by associating with each site of a two-dimensional lattice an n-dimensional unit length spin vector. The Hamiltonian for the $O(n)$ models is of the same form as that of the Heisenberg model,

$$H=-\sum_{\langle i,j\rangle}(\vec{\sigma}_i,\vec{\sigma}_j), \tag{1}$$

where the sum is over the nearest neighbor bonds $\langle i,j\rangle$ of the lattice and $(\vec{\sigma}_i,\vec{\sigma}_j)$ is the inner product of the unit vectors $\vec{\sigma}_i$ and $\vec{\sigma}_j$. For $n=2$, this model reduces to the so called two-dimensional XY model. It is well known [1] that this system cannot possess conventional long range order and this in literature is referred to as the Mermin-Wagner-Berezinski theorem. The system exhibits a second-order phase transition at the critical temperature T_c. Below T_c, the order parameter correlation function exhibits a quasi-long-range-order(QLRO), in which it decays algebraically with distance. This was well explained in terms of topological defects by Kosterlitz and Thouless [2], who demonstrated that vortex unbinding leads to the QLRO-disorder transition. The two-dimensional $O(3)$ model, on the other hand, is disordered at all finite temperatures. It may be noted that the system can have no stable topological defect as the spin vectors can point outside the plane [1].

In a nematic liquid crystal, one has spatially uncorrelated spins with the dominant interaction going like $-P_2(\cos\gamma_{ij})$, where γ_{ij} is the angle between the unit vectors $\vec{\sigma}_i$ and $\vec{\sigma}_j$ and P_2 is the second Legendre polynomial. A three-dimensional lattice model of the nematic was introduced by Lebwohl and Lasher [3], where the Hamiltonian can be written as

$$H=-\sum_{\langle i,j\rangle}P_2(\cos\gamma_{ij}), \tag{2}$$

$\langle i,j\rangle$ being the nearest neighbor pairs.

The model can easily be generalized to the n-component spins and this may be defined as the nematic n-vector model to distinguish it from the conventional n-vector model which we described earlier. It may be noted that in addition to the usual $O(n)$ symmetry, this model posseses the Z_2 symmetry, i.e., the directions $\vec{\sigma}(x)$ and $-\vec{\sigma}(x)$ are equivalent. The three-dimensional nematic liquid crystal is characterized by the existence of topologically stable defects which are known as disclination lines.

A two-dimensional nematic n-vector model with $n=3$, also called the RP^2 model, in the recent past has been the subject of Monte Carlo (MC) simulation by several groups of investigators. One of the most interesting features of the RP^2 model is the existence of topologically stable defects even in two dimensions. The order parameter space is the sphere S^2 with opposite points identified and the homotopy group is the integers modulo 2, i.e., $\Pi_1(RP^{n-1})=Z_2$ for $n\geqslant3$. Chiccoli *et al.* [4] investigated the system for lattice sizes ranging from 5×5 to 80×80 and found that the heat capacity is insensitive to the system size, whereas in a system exhibiting a true phase transition, systematic sharpening of the heat capacity is expected. The order parameter correlation function was found to decay algebraically in the low temperature phase and exponentially in the high temperature phase. Nothing conclusive about the nature of the phase transition emerged from this work. A more elaborate study of the sytem using Monte Carlo method was subsequently carried out by Kunz and Zumbach [5]. These authors found a strong evidence for a topological phase transition driven by condensation of defects. The transition was found to be associated with a divergence of correlation length and susceptibility and a cusp in the specific heat.

About two decades ago, Zannoni [6] proposed a generalization of the Maier-Saupe mean field theory of nematic liquid crystals. Besides, using the usual $P_2(\cos\theta_{ij})$ term of the orientational part of the anisotropic interactions between the molecules, the author also investigated the higher rank interactions like $P_M(\cos\theta_{ij})$ with $M=4,6$. The findings demonstrated that with increasing values of M, the nature of the transition becomes more markedly first order, in which the

entropy and the order parameter ($\langle P_2 \rangle$) at the transition increases. Subsequently, Monte Carlo simulations of a generalization of a three-dimensional Lebwohl-Lasher were carried out by Chiccoli *et al.* [4] and by Romano [7] for interactions of the type P_4 and P_6, respectively, and the findings are in agreement with the predictions of Zannoni [6]. This trend can be qualitatively understood in a mean field framework in the following manner. The mean field potential which is proportional to $P_M(\cos\theta)$, where θ is the angle between a molecule and the director and M even possesses $(M+2)/2$ minima for θ lying in the range $[0,\pi]$ and the minima at $\theta=0$ and π become narrower and steeper with increasing M. Thus, with increase in the rank of the interaction, there is a possibility for the molecules to get trapped in any of the $(M-2)/2$ local minima rather than being completely aligned along the director. A molecule may, however, eventually get ordered along the director when it suddenly jumps out of a local minimum trap to get into the $\theta=0$ or π position where the potential well is deeper.

More recently, Zhang *et al.* [8] and Priezjev *et al.* [9] have included a P_4 term in their study of the three-dimensional Lebwohl-Lasher model and have found that this makes the otherwise weak first-order nematic-isotropic transition stronger first order.

The above mentioned research for three-dimensional systems and, in particular, the extensive MC study of a two-dimensional system with P_2 interaction motivated us to take up the present work.

In a recent work [10], we reported a limited amount of numerical study of another two-dimensional $O(3)$ system where the spins on a square lattice interact with the nearest neighbors via a $-P_4(\cos\gamma_{ij})$ interaction, where P_4 is the fourth Legendre polynomial. The symmetry breaking pattern of the P_2 and P_4 interactions are identical and topologically both models have the same homotopy class. It is, therefore, of some interest to see if they behave similarly. Our initial results indicated that there is a marked difference in the behavior of the two models as the specfic heat was found to sharpen with the increase in lattice size. The free energy also exhibited a double-well structure which is indicative of a first-order phase transition. The statistics of our work was, however, not good enough to reveal the finer details of the scaling behavior of various thermodynamic quantities that one would expect to be obeyed in a first-order phase transition.

In this paper, we present the results of a more elaborate numerical study of the two-dimensional $O(3)$ model with the $-P_4(\cos\gamma_{ij})$ interaction. We have significantly improved on our previous work in terms of a bigger lattice size and greatly improved statistics and these resulted in different and interesting findings about the P_4 model. We may point out that the scaling behavior of some of the thermodynamic quantities which emerged from the present work are qualitatively different from what was reported in our previous work on the P_4 model.

II. THE DEFINITION OF THE THERMODYNAMIC QUANTITIES RELATED TO THE P_4 MODEL

The Monte Carlo simulation was carried out on a square lattice of dimension $L\times L$ with the three-dimensional spins located at each site and interacting with nearest neighbors via the Hamiltonian

$$H=-\sum_{i,j} P_4(\cos\gamma_{ij}). \tag{3}$$

The specific heat is given by

$$C_V^*=\frac{d}{dT^*}\langle H\rangle, \tag{4}$$

where T^* is the dimensionless temperature. C_V^* can also be evaluated from the energy fluctuation

$$C_V^*=\frac{(\langle H^2\rangle-\langle H\rangle^2)}{T^{*^2}}. \tag{5}$$

The conventional long range order parameter is given by

$$\langle P_2\rangle=\frac{1}{2}\langle 3\cos^2\theta-1\rangle, \tag{6}$$

where θ is the angle that a spin makes with the preferred direction of orientation and the average is over the entire sample. The next higher rank order parameter is defined as

$$\langle P_4\rangle=\frac{1}{8}\langle 35\cos^4\theta-30\cos^2\theta+3\rangle. \tag{7}$$

The order parameter susceptibility is defined in terms of the fluctuations of the order parameter $\langle P_2\rangle$

$$\chi=\frac{(\langle P_2^2\rangle-\langle P_2\rangle^2)}{T^*}. \tag{8}$$

The second rank pair correlation coefficient is defined as

$$G_2(r)=\langle P_2(\cos\theta_{ij})\rangle_r, \tag{9}$$

where i and j are two spins separated by a distance r.

The topological defects present in this model will be described using the approach followed by Kunz and Zumbach [5]. The unit spin vectors at two neighboring sites x and y are $\vec{\sigma}(x)$ and $\vec{\sigma}(y)$. One can always map these spins on the unit sphere S^2 and connect them by the shortest geodesic. Following this procedure and starting from a closed loop Λ on the lattice, one ends up in a loop on the manifold RP^2. The homotopy class of the map is given by

$$W(\Lambda)=\prod_{(xy)\in\Lambda}\mathrm{sgn}[\vec{\sigma}(x),\vec{\sigma}(y)]. \tag{10}$$

For $W(\Lambda)=+1$, the loop would enclose an even number of defects and for $W(\Lambda)=-1$, an odd number of defects. This definition, however, fails for the exceptional case when $[\vec{\sigma}(x),\vec{\sigma}(y)]$ vanishes.

It is possible to extend the above procedure to define the density of defects as

$$D=\frac{1}{2}[1-\langle W(\Lambda_1)\rangle], \tag{11}$$

where Λ_1 is a closed loop attached to a unit square on the lattice. It vanishes in the ground state and is expected to show an exponential increase like $\exp(-E_0/T^*)$ at low temperatures, E_0 being the activation energy of a pair of defects.

A topological order parameter which is a measure of the pairing of defects is defined in the following manner. With the periodic boundary conditions imposed, our two-dimensional lattice would look like a torus. The topological order parameter is defined as

$$\mu=\langle W(\Lambda_0)\rangle, \tag{12}$$

where Λ_0 is a circle enclosing the torus. At low temperatures, where few defects are expected to be present, μ should be nonzero and should vanish at high temperatures.

III. THE COMPUTATIONAL DETAILS

The Monte Carlo simulations were performed on square lattices of size L^2 for $L=10,20,40,80$, and 160. Instead of the conventional single spin-flip Metropolis algorithm, we use the cluster algorithm of Wolff [11]. The method is ergodic and satisfies the detailed balance condition. The algorithm runs as follows.

(1) A random unit vector $\vec{r}$ is taken and a spin flip $\vec{\sigma}_x \rightarrow \vec{\sigma}_x'$ is defined as

$$\vec{\sigma}_x'=\vec{\sigma}_x-2(\vec{\sigma}_x,\vec{r})\vec{r}. \tag{13}$$

(2) Bonds (x,y) of the lattice are activated with a probability

$$p(x,y)=1-\exp(\min\{0,\beta s_5\}), \tag{14}$$

where,

$$s_5=s_4[35(s_3^2-2s_4)-15],$$

$$s_4=s_1s_2(s_3-s_1s_2),$$

$$s_3=(\vec{\sigma}_x',\vec{\sigma_y}'),$$

$$s_2=(\vec{\sigma_y},\vec{r}),$$

$$s_1=(\vec{\sigma}_x',\vec{r}),$$

and a cluster of activated bonds is thus constructed.

(3) All spins in a cluster are now flipped according to $\vec{\sigma}_x \rightarrow \vec{\sigma_x}'$.

The various thermodynamic quantities were computed using the histogram reweighting technique of Ferrenberg and Swendsen [12]. Briefly the method works as follows. The partition function of the system is given by

$$Z(K)=\sum_S W(S)\exp[KS], \tag{15}$$

where $K=-1/K_BT$, K_B being the Boltzmann constant set equal to 1. $S=\Sigma_{i,j}P_4(\cos\gamma_{ij})$ is a function of the spins of the system and $W(S)$ is the density of states. Suppose that R Monte Carlo simulations have been performed at temperatures $K_n, n=1,\ldots,R$ and the data has been stored as histograms $\{N_n(S)\}$ with the total number of configurations is $n_n=\Sigma_{n=1}^R N_n$. If τ_n is the autocorrelation time, then we define a quantity $g_n=1+2\tau_n$. Then the essential multiple-histogram equation for the probability $P(S,K)$ is written as

$$P(S,K)=\frac{\sum_{n=1}^{R} g_n^{-1}N_n(S)\exp[KS]}{\sum_{m=1}^{R} n_m g_m^{-1}\exp[K_mS-f_m]}, \tag{16}$$

where the free energy f_n is given by

$$\exp\{f_n\}=\sum_S P(S,K_n). \tag{17}$$

The average value of any operator on S can be evaluated as a function of K from

$$\langle A(S)\rangle(K)=\sum_S A(S)P(S,K)/z(K), \tag{18}$$

where

$$z(K)=\sum_S P(S,K). \tag{19}$$

The values of f_n could be found self-consistently by iterating Eqs. (16) and Eq. (17). For all lattice sizes and for all temperatures; a straightforward iteration of these equations worked very satisfactorily.

When simulating an unknown system, one is always faced with two issues. The nature of the phase transition is first to be resolved and, subsequently, the various thermodynamic quantities are to be determined. The order of the phase transition can conveniently be determined by the method first proposed by Lee and Kosterlitz [13]. For a temperature driven first-order transition in a finite system of volume L^d with periodic boundary conditions the histogram of the energy distribution may be computed by Monte Carlo simulation to yield

$$N(E;\beta,L)=\aleph Z^{-1}(\beta,L)\Omega(E,L)\exp(-\beta E), \tag{20}$$

where $\beta=1/T$, $\aleph$ is the number of MC sweeps, Z is the partition function, and $\Omega(E,L)$ is the number of states of energy E. For the two-dimensional P_4 model, we have in-

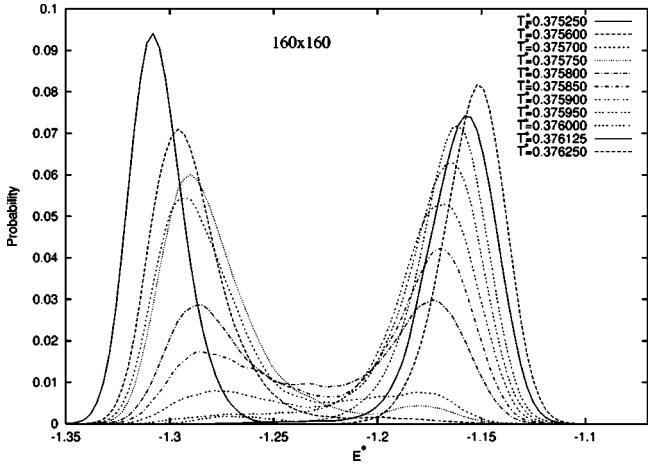

FIG. 1. The histograms for E^*, the average energy per particle generated for the 160×160 lattice for the P_4 model at 11 temperatures indicated.

vestigated that $N(E;\beta,L)$ has a characteristic double-peak structure in the neighborhood of T_c. The two peaks at $E_1(L)$ and $E_2(L)$ corresponding, respectively, to the ordered and disordered states are separated by a minimum at $E_m(L)$. We define a free-energy-like quantity

$$A(E;\beta,L,\aleph)\equiv-\ln N(E;\beta,L) \tag{21}$$

and the bulk free-energy barrier is defined as

$$\Delta F(L)=A(E_m;\beta,L,\aleph)-A(E_1;\beta,L,\aleph). \tag{22}$$

It may be noted that $A(E_1;\beta,L)=A(E_2;\beta,L)$ and ΔF is independent of $\aleph$. For a continuous transition, $\Delta F(L)$ is independent of L and for a first-order transition it is an increasing function of L. If one is in a region where L is sufficiently large so that $L\gg\xi$, where ξ is the correlation length [13], then ΔF obeys the scaling relation

$$\Delta F\sim L^{d-1}. \tag{23}$$

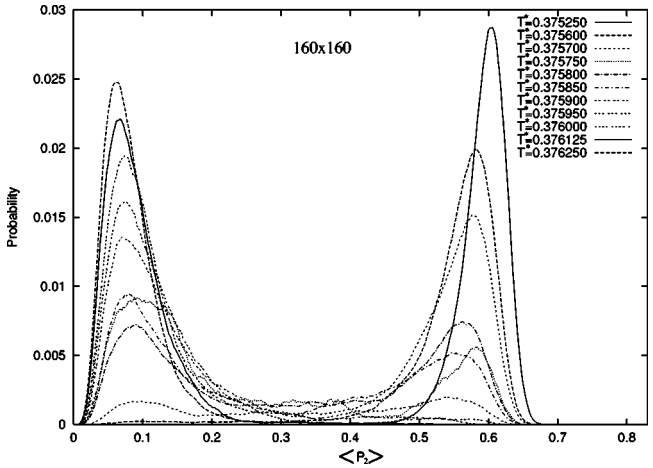

FIG. 2. The histograms for the order parameter $\langle P_2\rangle$ generated for the 160×160 lattice for the P_4 model at the temperatures indicated.

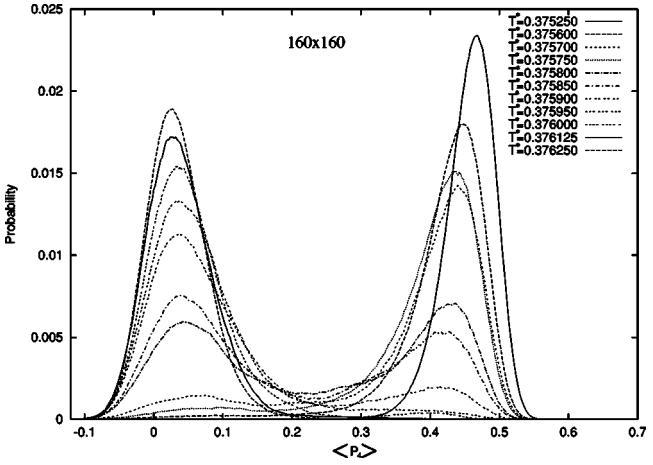

FIG. 3. The histograms for the order parameter $\langle P_4\rangle$ for the 160×160 lattice for the P_4 model at the temperatures indicated.

Clearly, the temperature at which the double-well structure of A has two equally deep minima gives a precise estimation of the transition temperature.

IV. RESULTS AND DISCUSSION

The MC simulations were performed for $L=10$, 20, 40, 80, and 160 using the cluster algorithm of Wolff described in the preceding section. For each lattice size, about 10–12 temperatures close to transition were chosen for the simulation. In Figs. 1–3, we have depicted the histograms generated for E^*, the average energy per particle, the order parameter $\langle P_2\rangle$ and the order parameter $\langle P_4\rangle$ for $L=160$. It is clear from the histograms that there is a temperature region where the MC sampling takes place between the ordered and the disordered phases. These diagrams are in sharp contrast to those obtained for the two-dimensional P_2 model for $L=80$ (Figs. 4 and 5) for energy and $\langle P_2\rangle$, respectively [14].

In Table I, we have presented the details of our simulation. For each lattice size, the simulations were carried out for the temperatures indicated. The number of Wolff clusters

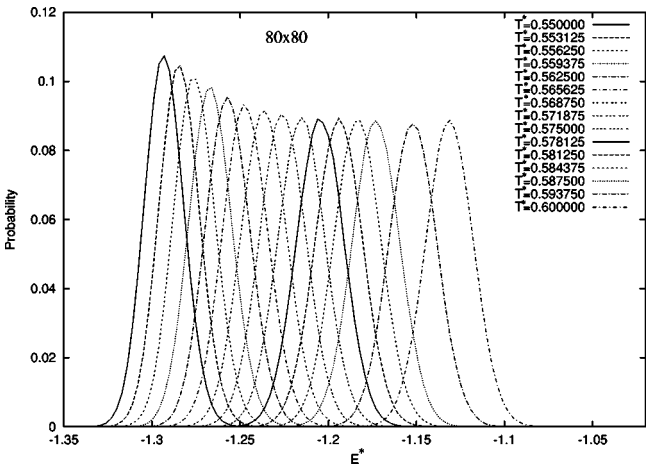

FIG. 4. The histograms for energy per particle E^* generated for the 80×80 lattice for the P_2 model [14] at 15 temperatures indicated.

TABLE I. T^* is the dimensionless temperature, L is the lattice size, n_c is the number of Wolff clusters, which for all lattices except 160×160 and at all temperatures is 10^9, $\langle c\rangle$ is the average cluster size, MCS is the number of equivalent Monte Carlo sweeps (see text) in units of 10^9, and τ is the autocorrelation time for energy (in units of Wolff clusters).

						$L=160$						
T^*	0.37525	0.3756	0.3757	0.37575	0.3758	0.37585	0.3759	0.37595	0.376	0.376125	0.37625	
n_c	10^9	5×10^9	5×10^9	10^{10}	5×10^9	5×10^9	10^9	10^9	10^9	10^9	10^9	
$\langle c\rangle$	17157	17095	17094	17079	16892	16848	16825	16796	16781	16763	16759	
MCS	0.670	3.338	3.338	6.671	3.299	3.219	0.657	0.656	0.655	0.654	0.654	
τ	3932	6154	182302	420000	190332	76334	48813	40000	11600	3596	2986	
						$L=80$						
T^*	0.37	0.372	0.374	0.375	0.37575	0.376	0.37625	0.3765	0.37675	0.377	0.378	0.38
$\langle c\rangle$	4569	4529	4461	4419	4367	4331	4269	4214	4183	4169	4114	4021
MCS	0.714	0.707	0.697	0.69	0.682	0.677	0.667	0.658	0.654	0.651	0.643	0.628
τ	204	261	617	1130	18806	33832	48653	16024	15958	7112	718	409
						$L=40$						
T^*	0.36	0.365	0.37	0.3725	0.375	0.376	0.377	0.37725	0.3775	0.37825	0.38	0.39
$\langle c\rangle$	1210	1195	1173	1159	1138	1130	1098	1092	1080	1052	1017	893
MCS	0.756	0.747	0.733	0.724	0.711	0.706	0.686	0.683	0.675	0.658	0.636	0.558
τ	86	104	168	267	1610	6400	7895	9097	5813	4497	645	73
						$L=20$						
T^*	0.35	0.36	0.37	0.375	0.378	0.38	0.383	0.39	0.41	0.43		
$\langle c\rangle$	315	311	303	295	287	280	263	236	179	123		
MCS	0.788	0.778	0.758	0.736	0.716	0.700	0.658	0.590	0.448	0.308		
τ	67	77	154	784	934	1157	853	171	32	17		
						$L=10$						
T^*	0.35	0.36	0.37	0.38	0.385	0.39	0.40	0.41	0.42	0.43		
$\langle c\rangle$	81	80	79	76	73	70	62	56	51	46		
MCS	0.810	0.800	0.790	0.760	0.730	0.700	0.620	0.560	0.510	0.460		
τ	61	96	134	191	246	247	145	68	38	21		

generated ranges from 10^9 to 10^{10} and the average cluster size for each temperature is also shown in the table. It is evident from the table that for a given lattice, the average size of the Wolff cluster decreases with increase in temperature. The maximum cluster size occurred for the smallest lattice, namely, 81.4% and this decreased with increase in the lattice size. For the $L=160$ lattice, the average cluster size varied from 67% to 65.5%, for the temperature range we studied. (It must, however, be noted that this may be due to a smaller temperature range over which the simulations were carried out for the larger lattices). We have also presented the equivalent number of MC sweeps and the autocorrelation time (in the number of Wolff clusters) in the

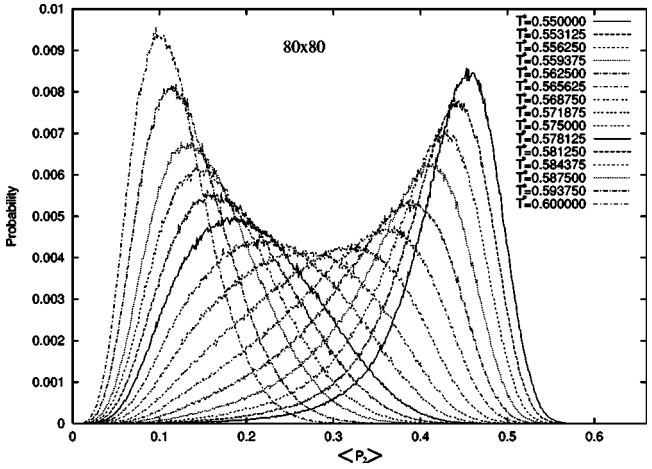

FIG. 5. The histograms for the order parameter $\langle P_2\rangle$ for the 80×80 lattice for the P_2 model [14] at the temperatures indicated.

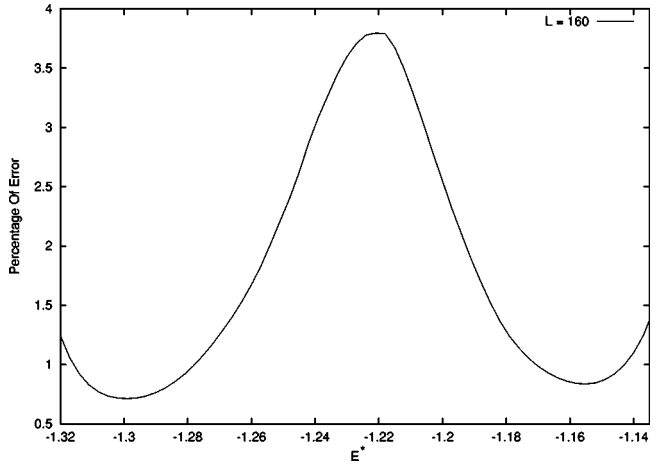

FIG. 6. The percentage error in the reweighted histograms plotted against E^* for $L=160$. The graph has been obtained using Eq. 24.

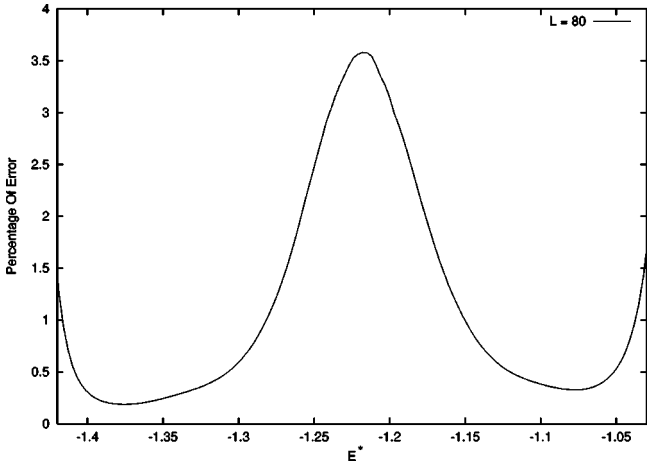

FIG. 7. The percentage error in the reweighted histograms plotted against E^* for $L=80$. The graph has been obtained using Eq. 24.

table. One MC sweep has been taken as the amount of computer run where all particles in a lattice have been on average flipped once. The autocorrelation time increases rapidly with the increase in lattice size and possesses a sharp maximum at the transition temperature.

The error in estimating the probability $P(S,K)$ in the histograms is given by

$$\delta P(S,K)=\frac{1}{\left[\sum_n g_n^{-1}N_n(S)\right]}P(S,K). \qquad (24)$$

This could be estimated directly from the histograms. The error is maximum for the largest lattice where the autocorrelation time is large. Figures 6 and 7 show the relative error in $P(S,K)$ for the lattices $L=80$ and 160. In the neighborhood of $E^*=-1.22$, the error has a peak value of about 3.5%,

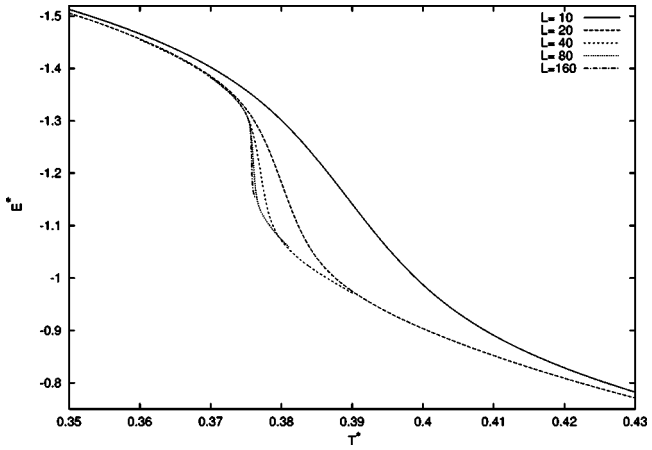

FIG. 8. The average energy per particle E^* plotted against the dimensionless temperature T^* for different lattice sizes. These graphs have been generated from the energy histograms shown in Fig. 1 using the multiple histogram reweighting (Eq. 15–18 of text). An idea of the error involved in these plots may be obtained from the error plots in Figs. 6 and 7.

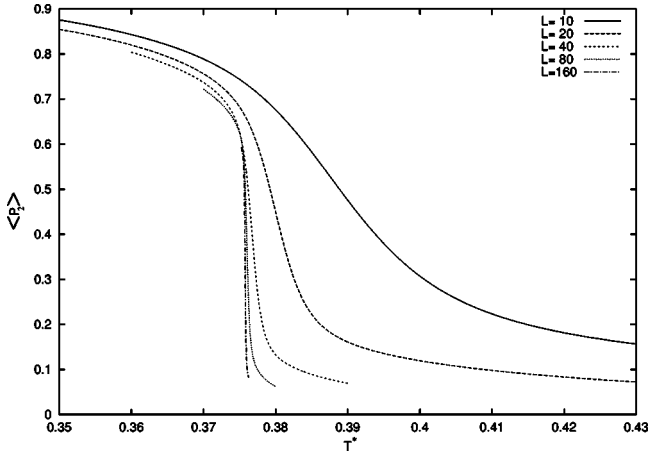

FIG. 9. The order parameter $\langle P_2\rangle$ plotted against temperature T^* for various lattice sizes. For comments on errors, please see Fig. 8.

whereas it is about 0.7% near the energies where the histograms have peaks. It may be pointed out that it will be a very difficult task to reduce the errors in the neighborhood of $E^*=-1.22$. This is evident because of the nature of the histograms (Fig. 1). The configurations generated have two more or less sharp peaks with relatively few configurations lying in the mid-range. Increasing the number of configurations further is unlikely to reduce the error in the region between the peaks by any significant amount.

The histogram reweighting of these results yielded the variation of energy and order parameters as functions of temperature (Figs. 8, 9, and 10). The reweighting technique of Ferrenberg and Swendsen was evoked also to generate the free-energy-like quantity A from the energy histograms and the free-energy barrier $\Delta F(L)$ could be obtained. A plot of free energy A vs energy E^* for different values of L is shown in Fig. 11, which clearly shows how the barrier height grows with L. The scaling relation Eq. (23) has been tested in Fig. 12 where ΔF has been plotted against L and a good linear fit has been obtained. It may be remarked that from the relation

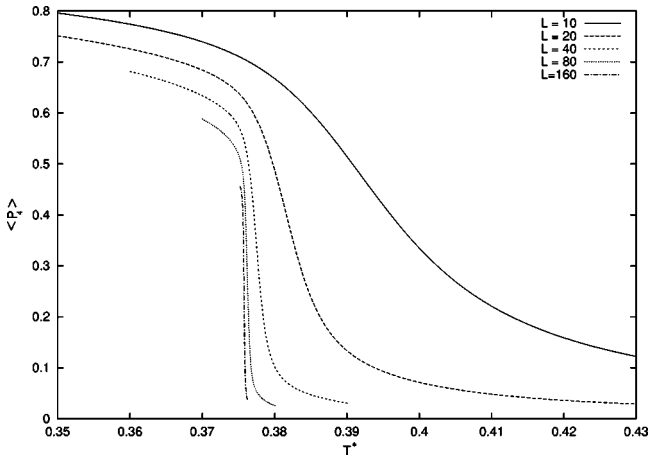

FIG. 10. The order parameter $\langle P_4\rangle$ plotted against temperature T^* for various lattice sizes. For comments on errors, please see Fig. 8.

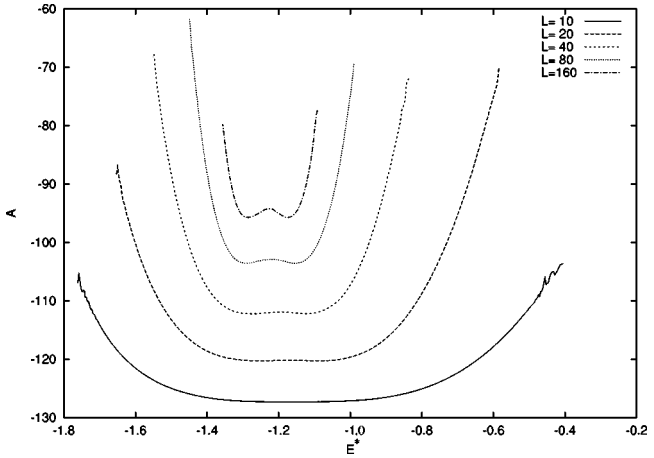

FIG. 11. The free energy A generated by the multiple histogram reweighting plotted against energy per particle E^* for different lattice sizes. The graphs are shifted vertically for clarity.

$\Delta F(\xi) \simeq 1$ we obtained the correlation length for our system of the order of 100 lattice spacings but the scaling relation is obeyed very well down to $L=20$.

The specific heat per particle C_V^* was obtained by two methods. The energy per particle E^* obtained from multiple histogram reweighting was fitted against temperature using a cubic spline and the derivative yielded C_V^* [Eq. (4)]. The other method is the conventional fluctuation relation given by Eq. (5). The two sets of results agreed within statistical error and Fig. 13 shows the variation of C_V^* with temperature for different values of L, where the sharpening of C_V^* at the transition is evident and may be contrasted with its behavior obtained for the two-dimensional P_2 model by other investigators [4,5]. The order parameter susceptibility was evaluated using Eq. (8) and its temperature variation for various values of L is shown in Fig. 14. We have found that the maxima of specific heat and susceptibility both scale as L^2 and the plots are shown in Fig. 15.

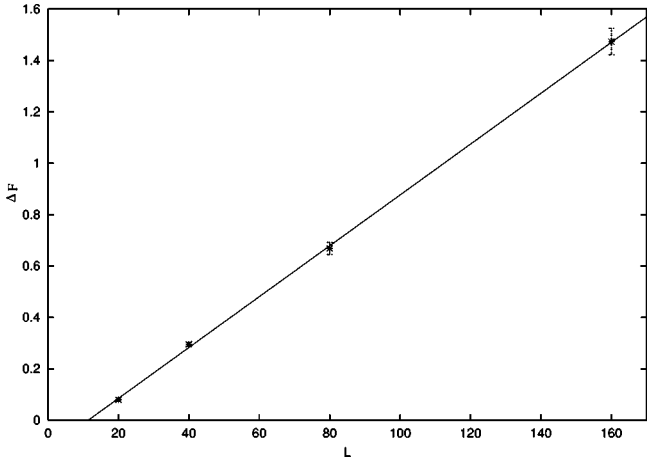

FIG. 12. The free-energy barrier height ΔF plotted against lattice size L with the linear fit represented by the straight line. (The error bars for two points are of the dimensions of the symbols used for plotting).

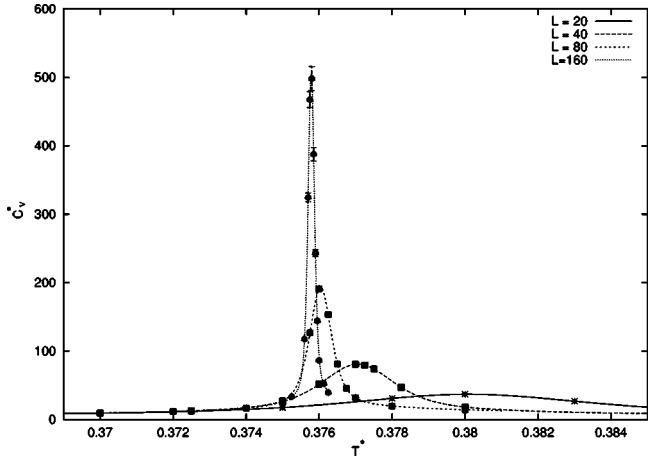

FIG. 13. The specific heat per particle C_V^* plotted against temperature T^* for different lattice sizes. (The error bars for most points are of the dimensions of the symbols used for plotting).

The finite size scaling relation

$$T_C(L) - T_C(\infty) \sim L^{-d} \tag{25}$$

for a first-order phase transition was tested. $T_C(\infty)$ is the thermodynamic limit of the transition temperature T_C which can be obtained in a number of ways. $T_C^{C_V}$ and T_C^{χ}, respectively, represent the transition temperatures obtained from the peak positions of the specific heat and the order parameter susceptibility, T_C^F represents the transition temperature obtained from the fine tuning of the free energy vs energy curve to obtain two equally deep minima, and finally $T_C^{P_2}$ represents the transition temperature obtained from the position of the peak of the derivative of the P_2 vs T curves obtained from histogram reweightings. Finally, $T_C^{P_4}$ represents the transition temperatures obtained from the peak position of the derivative of the P_4 vs T curves. In Fig. 16, we have plotted the transition temperatures obtained by these methods against L^{-2}. Expectedly, the slopes of these straight

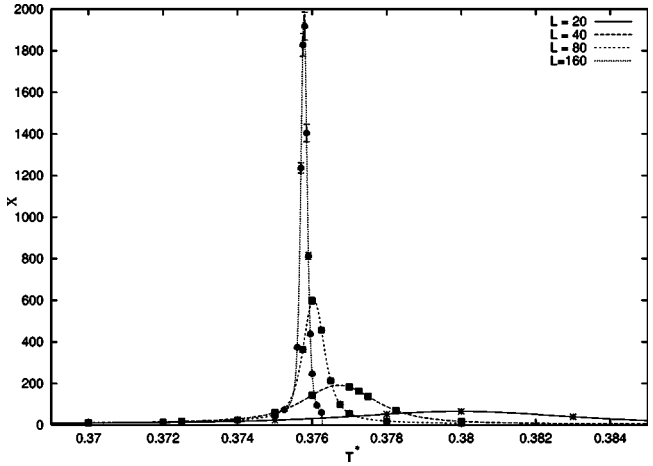

FIG. 14. The order parameter susceptibility χ plotted against temperature T^* for different lattice sizes. (The error bars for most points are of the dimensions of the symbols used for plotting).

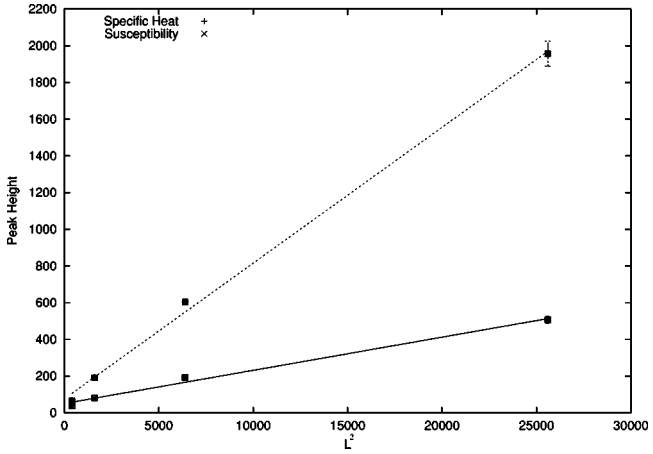

FIG. 15. The peak heights of specific heat per particle C_V^* and susceptibility χ plotted against L^2 with the linear fits represented by the straight lines. (Excepting one point, the error bars are of the size of the symbols used for plotting).

lines are marginally different but they all, in the thermodynamic limit $L\to\infty$, converge to within a value 0.376 ± 0.015. We have also estimated the pseudospinal temperatures of the system for $L=160$ from fine tuning of the temperature and observation of the free energy vs energy curve. The temperatures are $T^+=0.3764$ and $T^-=0.3749$, respectively.

The pair correlation function $G_2(r)$ given by Eq. (9) has been plotted in Fig. 17 for $L=80$ at $T^*=0.37$, 0.374, 0.37575, and 0.3765 and in Fig. 18 for $L=160$ at $T^*=0.37525$, 0.3757 and 0.3759. For temperatures lower than the transition temperature, $G_2(r)$ could be fitted accurately to the power law decay to a plateau, $(ar^{-p}+c)$. For $L=80$ at $T^*=0.374$ we obtained $p=0.529$ and $c=0.466$, whereas for $L=160$ at $T^*=0.37525$ we had $p=0.522$ and $c=0.316$. For temperatures just above the transition, c vanished and p for both lattices was found to be 0.5. It may be noted that the parameter c is nothing but the asymptotic value of the pair correlation function and our simulation reveals that it is very close to the square of the long range order parameter $\langle P_2\rangle$ at the respective temperatures.

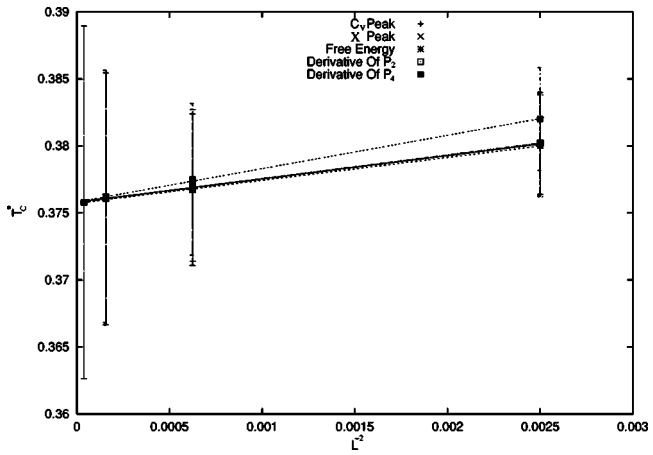

FIG. 16. The transition temperature T_c^* obtained from (a) specific heat peak position, (b) susceptibility peak position, (c) fine tuning of free energy curve, (d) peak position of the derivative of $\langle P_2\rangle$, and (e) peak position of the derivative of $\langle P_4\rangle$ plotted against L^{-2} along with the respective linear fits. The intercept on the y axis is 0.376 ± 0.015.

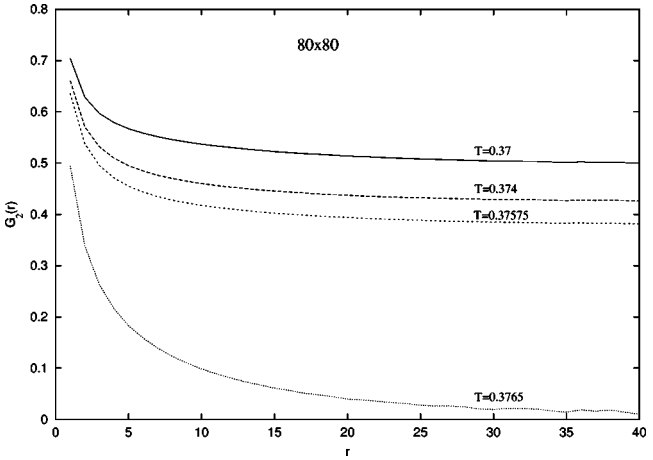

FIG. 17. The plots of the pair correlation function $G_2(r)$ against r for the 80×80 lattice for the temperatures indicated. The curves are plotted for r ranging up to $L/2$.

We now turn to the topological quantities. The density of defects are plotted in Fig. 19 and shows an increase above the transition temperature. The derivative dD/dT^* is plotted in Fig. 20 and it may be noted that this quantity rapidly sharpens with increase in lattice size. Quantitatively, dD/dT^* scales as L, as shown in Fig. 21. We may recall that Holm and Janke [15] in a recent study have found in the case of the three dimensional Heisenberg model that the density of defects behaves qualitatively like energy and its temperature derivative like the specific heat, which are not in agreement with our finding. The density of defects vanishes in the ground state and shows an exponential behavior exp $(-E_0/T^*)$ at low temperatures, E_0 being the activation energy for a pair of defects. For the 80×80 lattice, we have plotted the density of defects vs temperature in Fig. 22 which

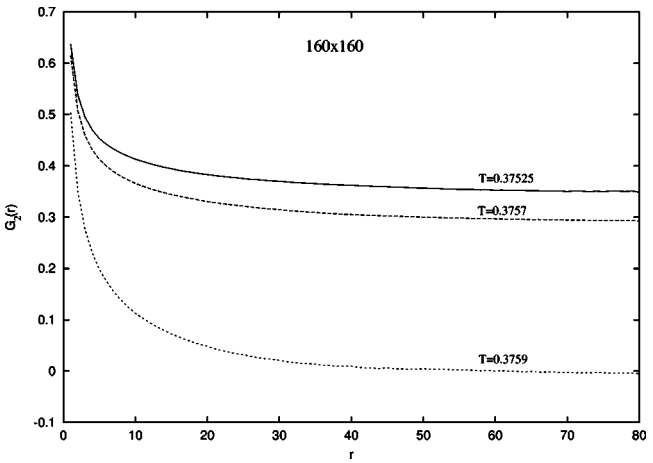

FIG. 18. The plots of the pair correlation function $G_2(r)$ against r for the 160×160 lattice for the temperatures indicated. The curves are plotted for r ranging up to $L/2$.

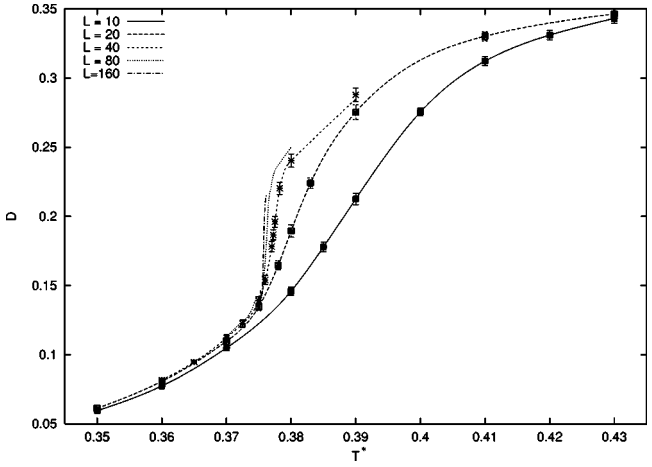

FIG. 19. Plots of density of defects D with temperature T^* for different lattice size L. (The error bars for most points are of the dimensions of the symbols used for plotting).

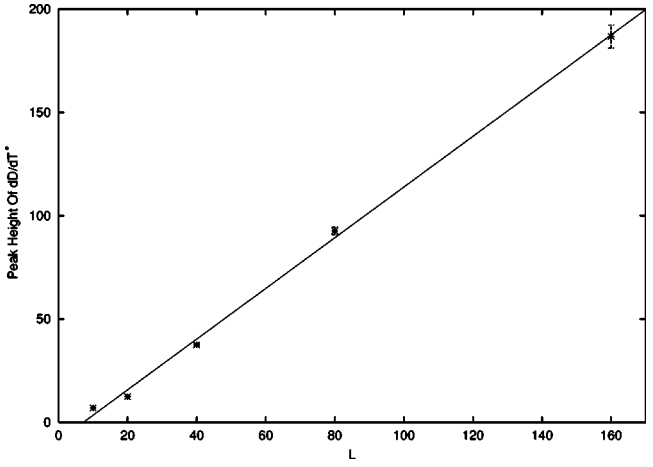

FIG. 21. The peak height of dD/dT^* curves plotted against lattice size L and the linear fit. (Excepting one point the error bars are of the size of the symbols used).

yields $E_0 = 2.93$ which is almost an order of magnitude greater than that obtained for the P_2 model by Kunz and Zumbach [5].

The topological order parameter is denoted by μ. It is nonzero at low temperatures and vanishes at T_c^*. A quantity $(1-\mu)/2$ is plotted against temperature in Fig. 23 for lattice size up to 40×40. These clearly show that defects play a dominant role in the phase transition exhibited by our model.

The autocorrelation time τ of energy was obtained by using the method proposed by Madras and Sokal [16] and were found to be some orders of magnitude greater than that for the P_2 model. Table I lists the autocorrelation time for different temperatures for different L. It is evident that τ shows a sharp increase in the neighborhood of the transition temperature. The plot of $\ln\tau$ vs L is shown in Fig. 24 and quantitatively we found that τ at T_C scales with an exponent L^{ϕ} where we obtained $\phi=2.7$.

V. CONCLUSION

It may be concluded that the present work which involves extensive Monte Carlo simulation reveals that the planar lattice model with three-dimensional spins interacting with the nearest neighbors with the P_4 interaction exhibits a strong first-order phase transition. This is remarkably different from the behavior of the other two-dimensional models which have been thoroughly investigated. The XY model and the nematic P_2 model exhibit second-order phase transition while the $O(3)$ Heisenberg model does not exhibit any transition at all. The sharpening of the specific heat with increase in lattice size and the agreement obtained with the various first-order scaling laws are in sharp contrast to the behavior of the planar P_2 model. It may be noted that the symmetry breaking pattern of both models are the same and both transitions are driven by topological defects.

From the nature of the variation of the autocorrelation time with lattice size and temperature, we may comment that in the planar P_4 model, the Wolff algorithm does not seem to reduce critical slowing down by any significant amount as it does to other $O(3)$ models. Usually, a cluster algorithm fails

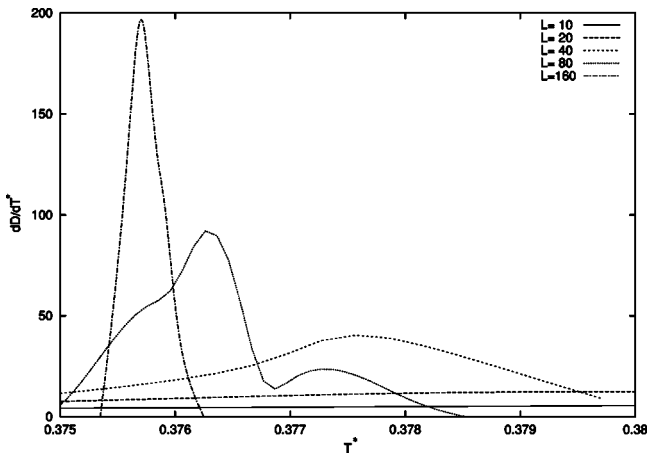

FIG. 20. The derivative dD/dT^* plotted against T^* for different lattice sizes.

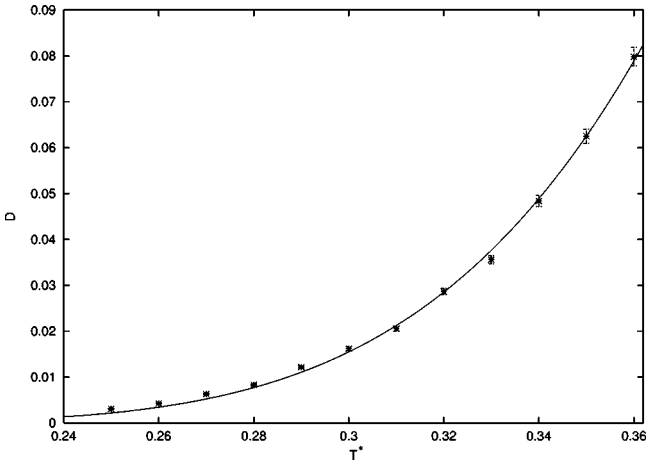

FIG. 22. Density of defects D plotted against T^* for $L=80$ lattice. The continuous curve represents the function $a\exp(-E_0/T^*)$, where the constants are $a=269.33$ and $E_0=2.929$. (The error bars for most points are of the dimensions of the symbols used for plotting).

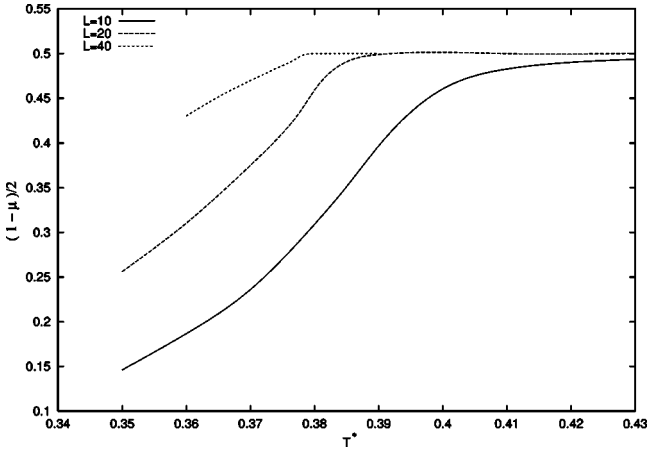

FIG. 23. Plots of a quantity $(1-\mu)/2$ with temperature T^* for different lattice size L.

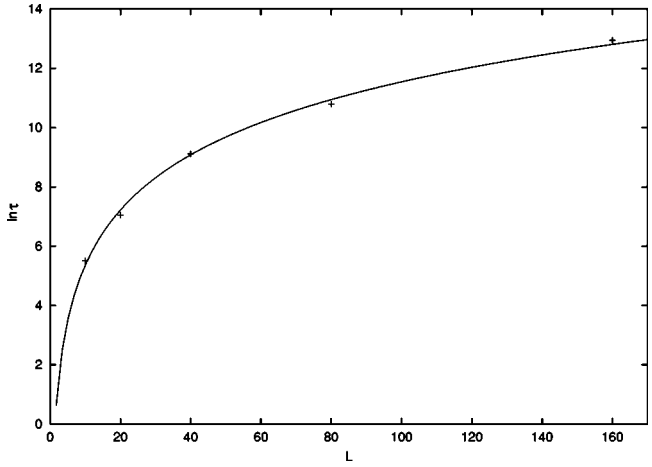

FIG. 24. Logarithmic plot of the peak value of autocorrelation time against L.

to result in efficient sampling when the cluster size for a given system is either too small or too large. It is evident from our work why the Wolff algorithm does not work for this model. The reason is that the transition is a thermal first-order one. For a thermal first-order transition, the clusters are either too big (comparable to the magnetization or the order parameter of the ordered phase) if the system is in one of the ordered phases or too small (comparable to the correlation length) if the system is in the disordered phase. As a result, the time to go between ordered phases and the disordered phase is very long. The autocorrelation time in the case of a planar P_2 interaction behaves in a completely different manner. Apart being significantly smaller than that in the P_4 model, it does not exhibit a peak at any temperature and increases monotonically. For example, in an 80×80 lattice in the P_2 model, τ varies from 24 to 768 when the reduced temperature changes from 0.5125 to 0.7 [14].

ACKNOWLEDGMENTS

We acknowledge the computer facility made available to us at the ICOSER center (Level III computer facility of DST) at the IACS, Calcutta.

[1] P. M. Chaikin and T. C. Lubensky, *Principles of Condensed Matter Physics* (Cambridge University Press, Cambridge, U.K., 1995).
[2] J.M. Kosterlitz and D.J. Thouless, J. Phys. C **6**, 1181 (1973).
[3] P.A. Lebwohl and G. Lasher, Phys. Rev. A **6**, 426 (1972).
[4] C. Chiccoli, P. Pasini, and C. Zannoni, Physica A **148**, 298 (1988).
[5] H. Kunz and G. Zumbach, Phys. Rev. B **46**, 662 (1992).
[6] C. Zannoni, Mol. Cryst. Liq. Cryst. Lett. **49**, 247 (1979).
[7] S. Romano, Liq. Cryst. **16**, 1015 (1994).
[8] Z. Zhang, M.J. Zuckermann, and O.G. Mouritsen, Mol. Phys. **80**, 1195 (1993).
[9] N.V. Priezjev and R.A. Pelcovits, Phys. Rev. E **64**, 031710 (2001).
[10] K. Mukhopadhyay, A. Pal, and S.K. Roy, Phys. Lett. A **253**, 105 (1999).
[11] U. Wolff, Phys. Rev. Lett. **62**, 361 (1989); Nucl. Phys. B **322**, 759 (1989).
[12] A.M. Ferrenberg and R.H. Swendsen, Phys. Rev. Lett. **61**, 2635 (1988); **63**, 1195 (1989).
[13] J. Lee, J.M. Kosterlitz, Phys. Rev. B **43**, 3265 (1991); Phys. Rev. Lett. **65**, 137 (1990).
[14] E. Mondal and S. K. Roy (unpublished).
[15] C. Holm and W. Janke, J. Phys. A **27**, 2553 (1994).
[16] N. Madras and A.D. Sokal, J. Stat. Phys. **50**, 109 (1988).